

Supplementary Information

Tetrazole-based Porous metal-organic frameworks for selective CO₂ adsorption and isomerization studies

Rui Zhang,^a De-Xian Meng,^a Fa-Yuan Ge,^b Jv-Hua Huang,^a Li-Fei Wang,^a Yong-Kai Xv,^a Xing-Gui Liu,^a Mei-Mei Meng,^a Hong Yan,^c Zhen-Zhong Lu,^{*a} He-Gen Zheng,^{*b} Wei Huang^{*a,d}

- a. Key Laboratory of Flexible Electronics (KLOFE) & Institute of Advanced Materials (IAM), Nanjing Tech University (NanjingTech), 30 South Puzhu Road, Nanjing 211800, China.
- b. State Key Laboratory of Coordination Chemistry, School of Chemistry and Chemical Engineering, Collaborative Innovation Center of Advanced Microstructures, Nanjing University, Nanjing 210023, P. R. China.
- c. 23rd Middle School of Daqing city, No. 385 Jingsan street, Sartu District, 163000, Daqing city, China
- d. Institute of Flexible Electronics (IFE), Northwestern Polytechnical University (NPU), 127 West Youyi Road, Xi'an 710072, China

Table S1. Crystal and Structure Refinement Data for compound **1**, **2** and **3**.

	1	2	3
Empirical formula	C ₈₄ H ₆₂ Cl ₁₆ Cu ₁₂ N ₅₈ O ₁₆	C ₃₃ H ₂₅ Cu ₃ ON ₃₈	C ₁₀ H ₆ CuN ₁₂
Formula weight	3469.72	1160.53	357.81
Temp. (K)	291	295	296
MoK _a	0.71073	0.71073	0.71073
Crystal system	Cubic	Triclinic	Monoclinic
Space group	<i>Fm-3c</i>	<i>P</i> -1	<i>P</i> 2 ₁ /c
<i>a</i> , Å	60.758(1)	9.279(1)	9.715(1)
<i>b</i> , Å	60.758(1)	12.302(2)	6.900(1)
<i>c</i> , Å	60.758(1)	12.377(2)	9.955(1)
<i>a</i> (°)	90.00	61.304(3)	90
<i>β</i> (°)	90.00	86.912(3)	90.104(3)
<i>γ</i> (°)	90.00	88.272(4)	90
<i>V</i> , Å ³	224291.4(5)	1237.6(4)	667.3(1)
Z	24	1	2
<i>ρ</i> _{calc} Mg/m ³	-	1.557	1.781
<i>μ</i> , mm ⁻¹	0.810	1.350	1.658
F(000)	41280	584	358
Refl. collected	322062	6201	4557
Independent refl.	8850/6309	4299/2859	1293/1229
Final R indices (R1)	0.0557	0.0638	0.0259
(all data) wR2	0.1290	0.1538	0.0855
GOOF	1.025	0.985	1.045

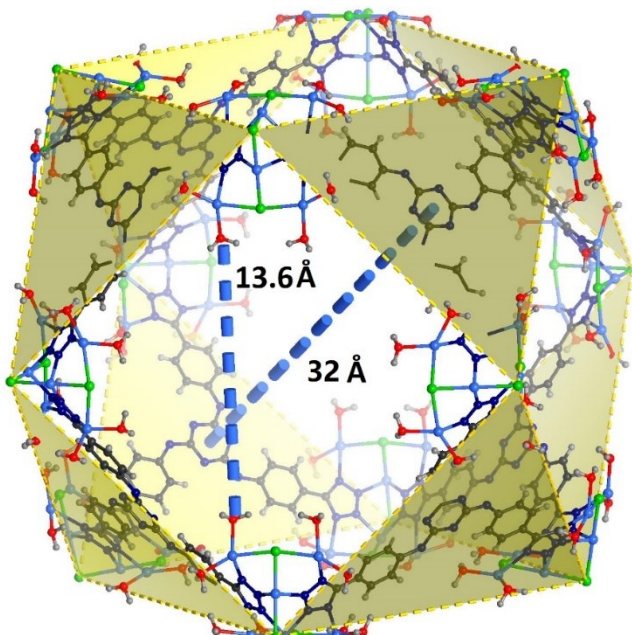


Figure S1. Truncated cube-shaped cages with square-shaped windows formed in **1**, the largest separation between octahedrons is 32 Å, the square-shaped windows is 13.6×13.6 Å taking *van der waals* radii into consideration (Cu, light blue; C, black; H, grey; N, dark blue; O, red; Cl, green).

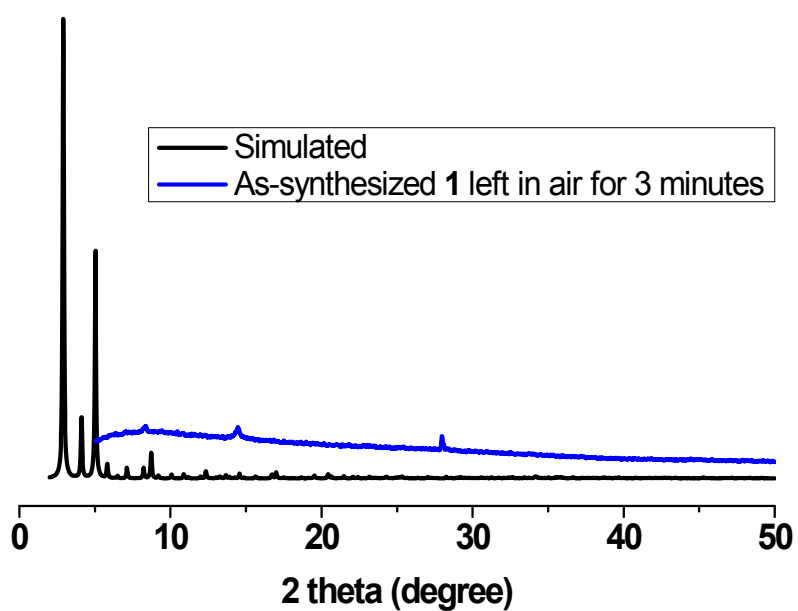
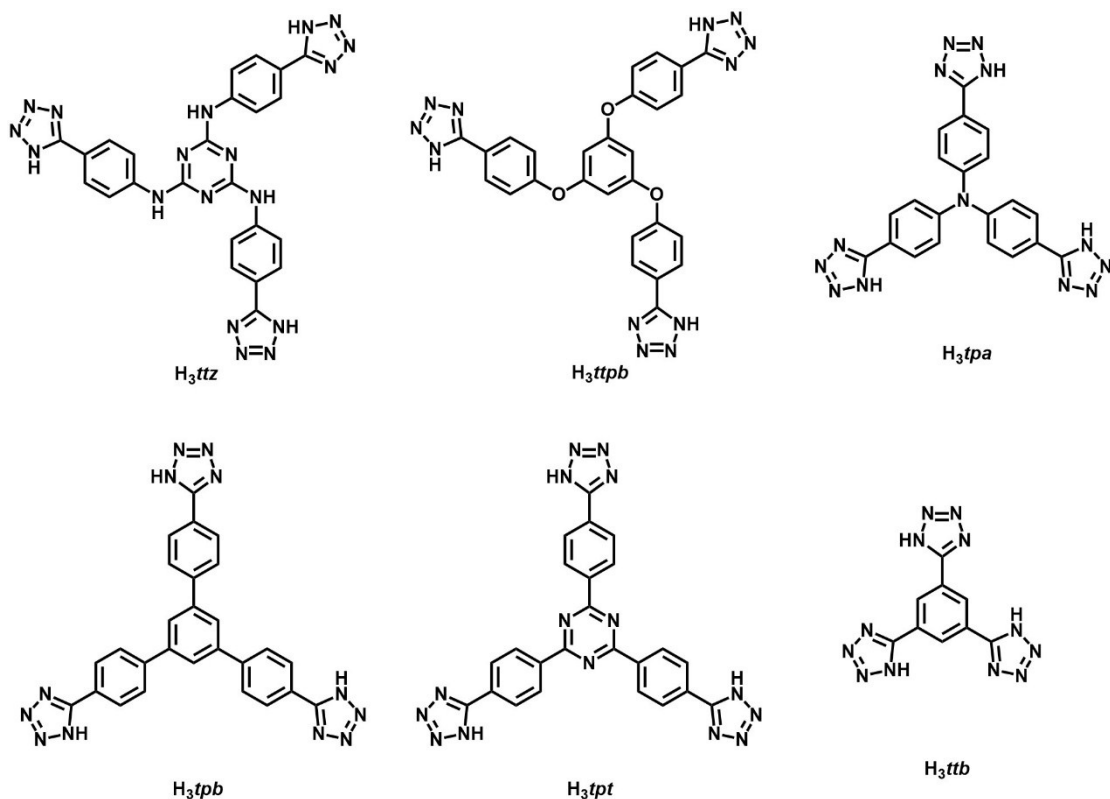


Figure S2. The PXRD patterns of simulated and as-synthesized crystals left in air for 3 minutes of **1** (the porous structure of **1** collapse upon losing solvent guests when left in air).



Scheme S1. All the tri-topic tetrazolate ligands used in this and reported work.

Table S2. Summary of MOFs based on tri-topic tetrazole-based ligands and transitional metals.

Ligand ^a	Metal	Space group	Structure	Reference
<i>ttz</i>	Cu ^{II}	<i>F m-3c</i>	3D framework of ‘the’ topology	this work
<i>tpa</i>	Mn ^{II}	<i>R -3c</i>	double layer	[1]
<i>ttpb</i>	Cu ^{II} , Cd ^{II}	<i>R -3</i>	double layer	[2]
<i>tpb</i>	Cu ^{II}	<i>P m-3m</i>	3D framework of ‘the’ topology	[3]
<i>tpt</i>	Cu ^{II} , Mn ^{II}	<i>I m-3m</i>	3D framework of ‘the’ topology	[3]
<i>btt</i>	Cu ^{II} , Mn ^{II} , Cr ^{II} , Fe ^{II} , Ni ^{II} , Co ^{II} , Cd ^{II} , Zn ^{II}	<i>P m-3m</i>	3D framework of ‘the’ topology	[4-10]

^a A diagram of these ligands is shown in Scheme S1.

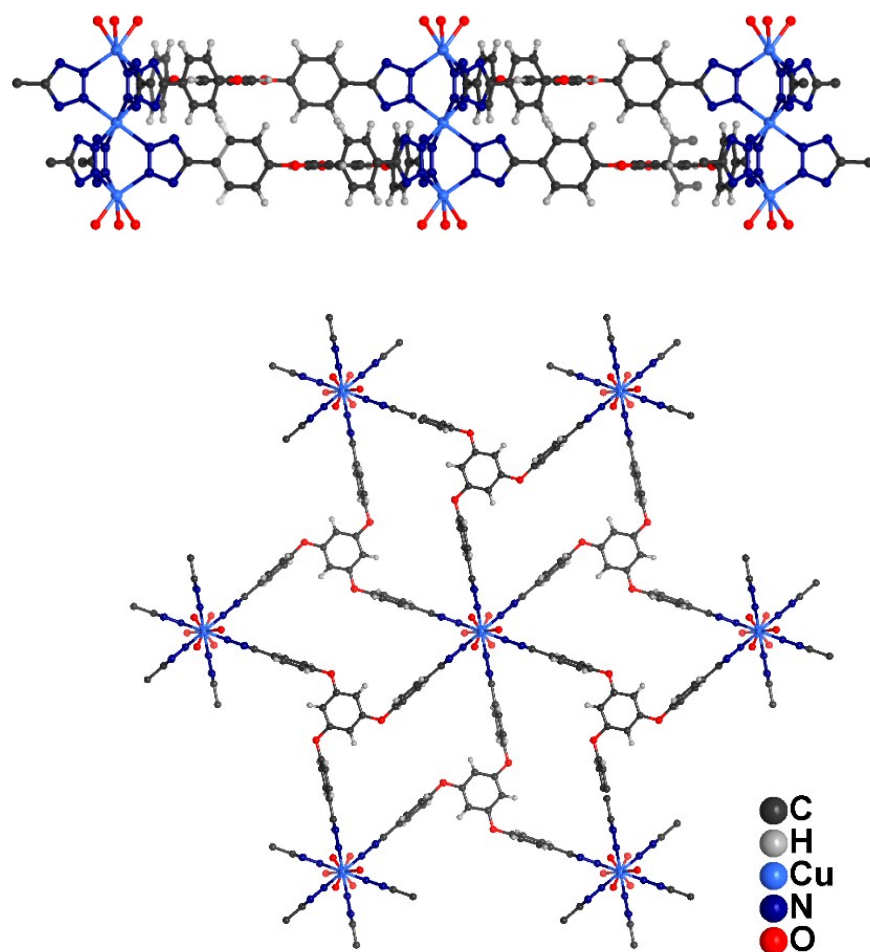


Figure S3. Side view and top view of the layer structure of **JUC-130**.

Table S3. A summary of reported MOFs based on *pmtz* ligand and transition metals.

	2	3	4R	5R[§]	6R	7R	8R
Formula	$\text{Cu}_3(\text{pmtz})_6 \cdot \text{DMF}$	$\text{Cu}(\text{pmtz})_2$	$\text{Co}(\text{pmtz})_2$, $\text{Fe}(\text{pmtz})_2$, $\text{Ni}(\text{pmtz})_2$, $\text{Zn}(\text{pmtz})_2$	$\text{Cu}_2(\text{pmtz})_3 \cdot \text{H}_2\text{O}^{\$}$	$\text{Cu}_4(\text{pmtz})_4$	$\text{Cd}(\text{pmtz})_2$	$\text{Cd}(\text{pmtz})_2$
Crystal system	Triclinic	Monoclinic	Orthorhombic	Trigonal	Orthorhombic	Tetragonal	Tetragonal
Space group	<i>P</i> -1	<i>P</i> 2 ₁ / <i>c</i>	<i>P</i> <i>bca</i>	<i>R</i> -3 <i>c</i>	<i>P</i> <i>bca</i>	<i>P</i> 4 ₂ / <i>nnm</i>	<i>I</i> 4 ₁ / <i>amd</i>
<i>a</i> , Å	9.279(1)	9.715(1)	8.229(6)	17.967(3)	20.535(6)	9.055(3)	6.469(3)
<i>b</i> , Å	12.302(2)	6.900(1)	9.348(7)	17.967(3)	12.631(4)	9.055(3)	6.469(3)
<i>c</i> , Å	12.377(2)	9.955(1)	17.89(1)	42.438(9)	11.271(3)	15.780(1)	32.80(3)
<i>α</i> (°)	61.304(3)	90	90	90	90	90	90
<i>β</i> (°)	86.912(3)	90.104(3)	90	90	90	90	90

γ (°)	88.272(4)	90	90	120	90	90	90
V , Å ³	1237.6(4)	667.3(1)	1377.1(8)	11864(1)	2923(1)	1294.1(1)	1372.8(1)
Z	1	2	4	6	4	4	4
Porous/non porous	27%	nonporous	nonporous	25%	nonporous	nonporous	nonporous

§ The copper atom in **5R** is not Cu^{II}, the valence state was not reported.

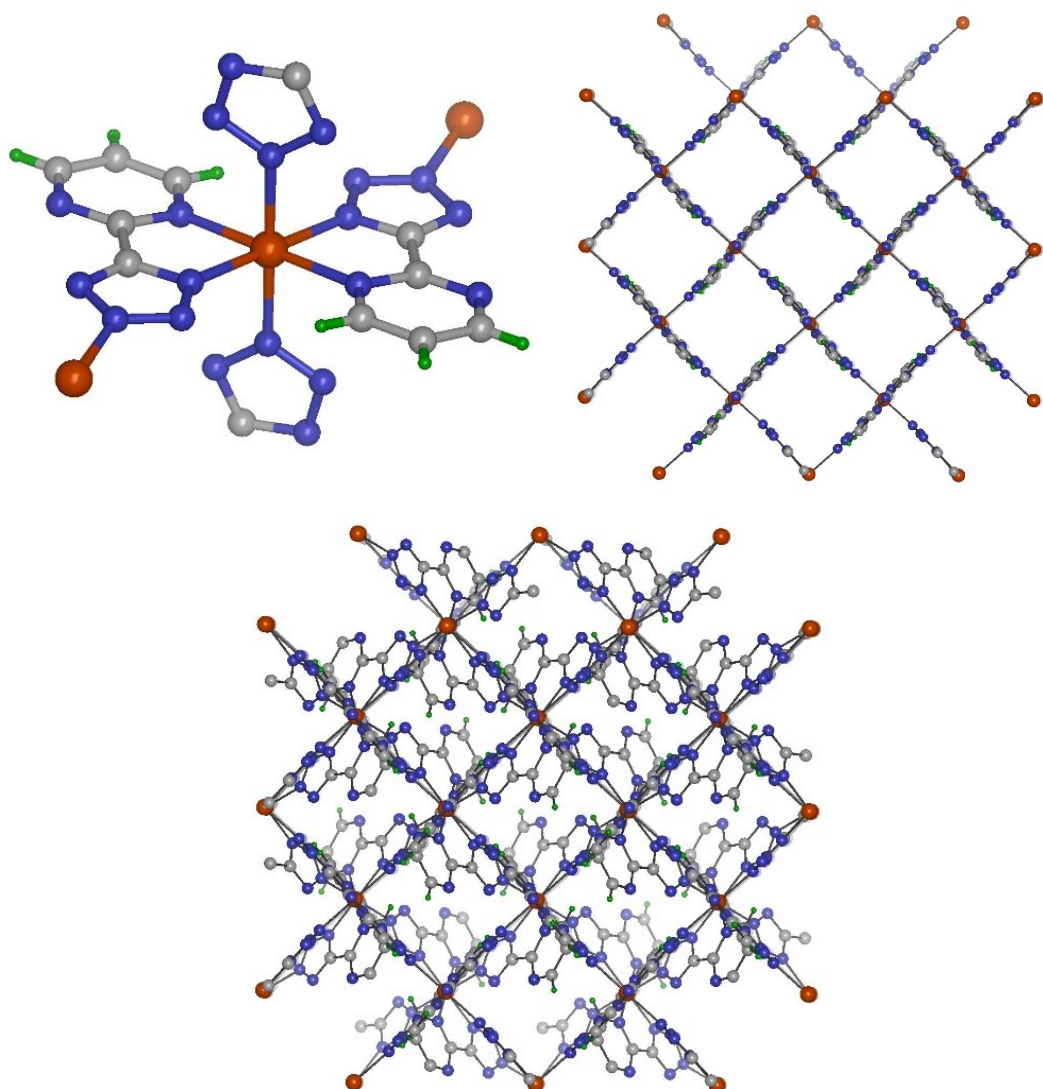


Figure S4. Top left: Coordination environment of metal center in **4R**. Top right: Layer structure in **4R** with adjacent *pmtz* molecules orthogonal to each other. Bottom: The packing of layers in **4R** (metal, brown; C, grey; H, green; N, dark blue).

Table S4. A summary of metal-nitrogen bond lengths in **2**, **3**, and **4R**.[§]

	2	3	4R			
	Cu(<i>pmtz</i>) ₂	Cu(<i>pmtz</i>) ₂	Zn(<i>pmtz</i>) ₂	Co(<i>pmtz</i>) ₂	Fe(<i>pmtz</i>) ₂	Ni(<i>pmtz</i>) ₂
B.L. ^a (Å)	2.394, 2.422	2.518	2.193	2.129	1.968	2.089
B.L. ^e (Å)	1.958~2.091	1.985~2.055	2.114~2.169	2.090~2.149	1.958~1.995	2.054~2.098

[§] Please find related references in the main text.

B.L.^a = Bond length in the axial direction; B.L.^e = Bond length in the equatorial plane.

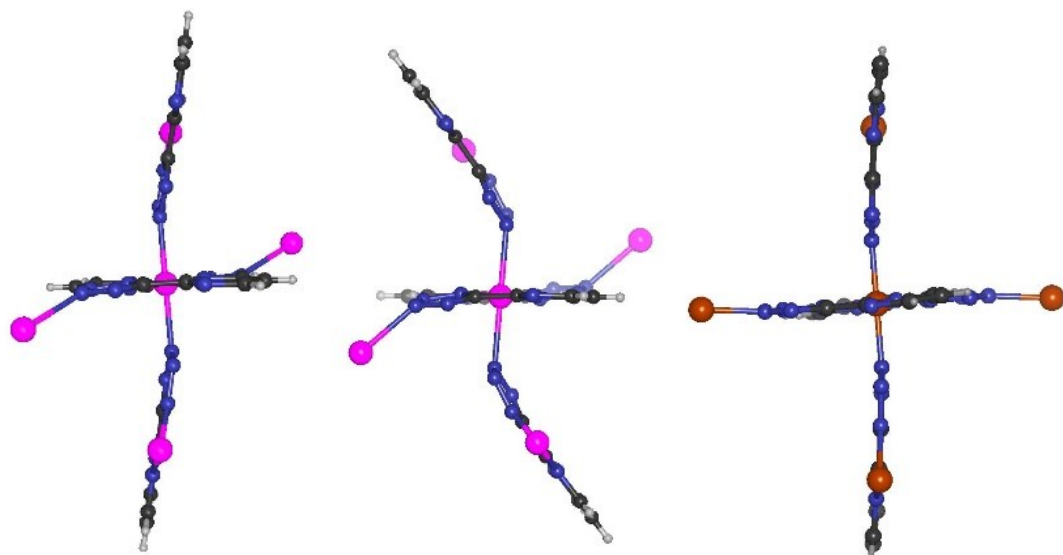
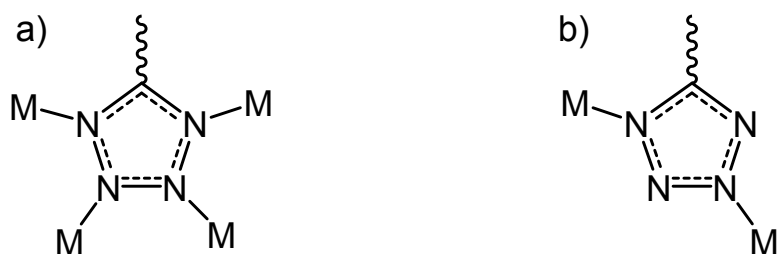


Figure S5. Left: There are *pmtz* ligands in the in-plane and ligands in the out-of-plane mode in **2**. Middle: *pmtz* ligands are all in the out-of-plane mode in **3**. Right: *pmtz* ligands are all in the in-plane mode in **4R**. (C, dark grey; H, light grey; N, indigo; O, red; Cu, purple, metal in **4R**, brown)



Scheme S2. Coordination modes of tetrazole group in **1** (a), **2** and **3** (b). (M is for metal).

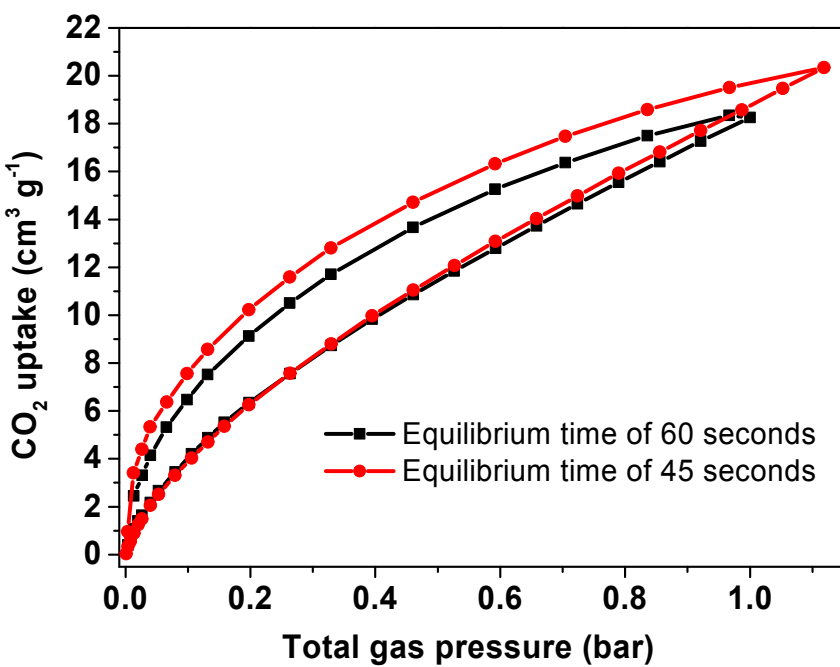


Figure S6. Isotherms of CO₂ for **2** collected using the equilibrium time of 45 and 60 seconds (Hysteresis loop was observed in both isotherms but became smaller as equilibrium time increase, this fact proved that the hysteresis was cause by slow equilibration of CO₂ in the adsorbing and desorbing processes).

IAST Analysis of the selectivity data in compound 2.

Ideal adsorbed solution theory (IAST)¹¹ was used to determine the selectivity factor, *S*, for binary mixtures using pure component isotherm data. The selectivity factor, *S*, is defined according to Equation 1 where *x_i* is the amount of each component adsorbed as determined from IAST and *y_i* is the mole fraction of each component in the gas phase at equilibrium. The IAST adsorption selectivities were calculated for CO₂/N₂ binary mixtures of compositions (50:50) at 273 K and a total pressure of 1.0 bar.

$$S = \frac{x_1/y_1}{x_2/y_2} \quad (1)$$

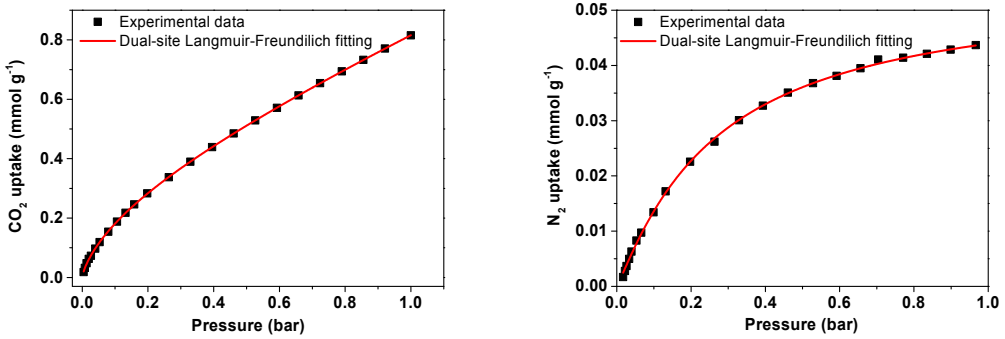


Fig. S7. The dual-site Langmuir-Freundlich fitting for CO₂ and N₂ adsorption isotherms in **2** at 273 K.

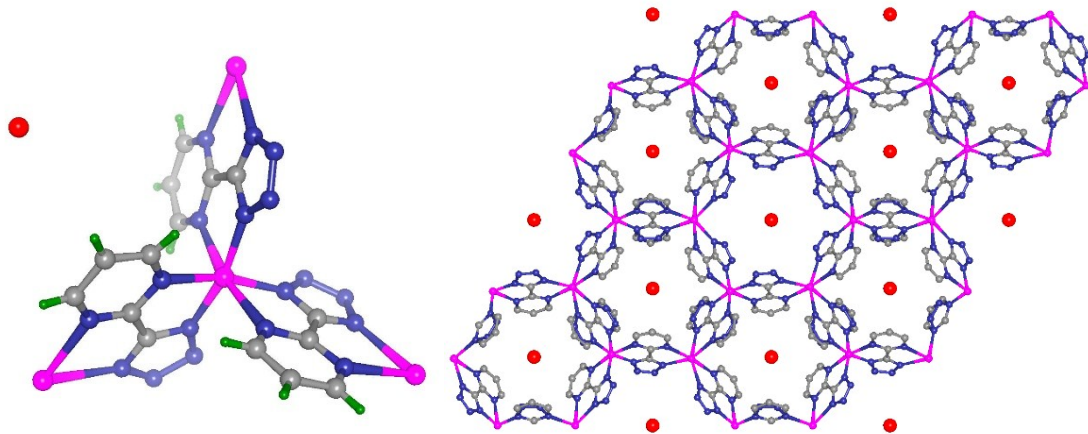
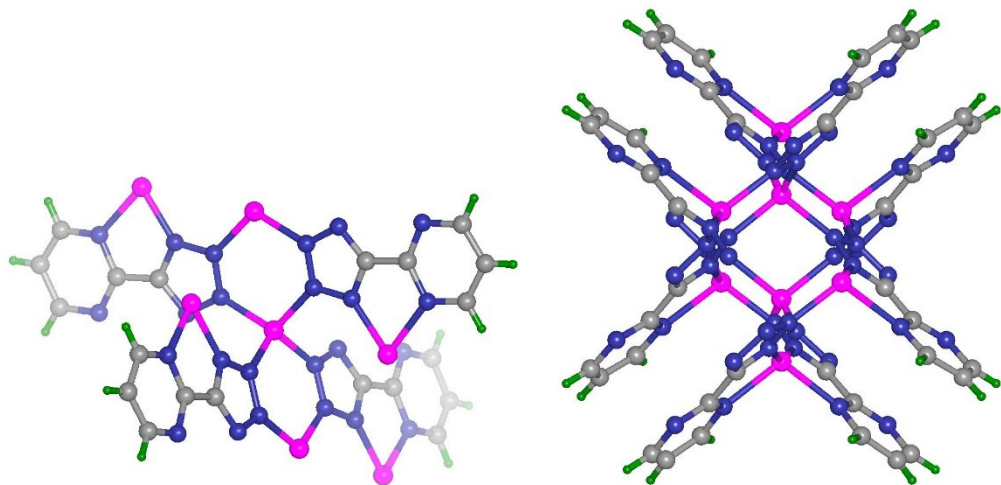


Figure S8. Coordination environment of copper atom in **5R**, Cu₂(pmtz)₃·H₂O. Right: Layer structure in **5R** (Cu, purple; C, grey; H, green, N, dark blue; O, red).



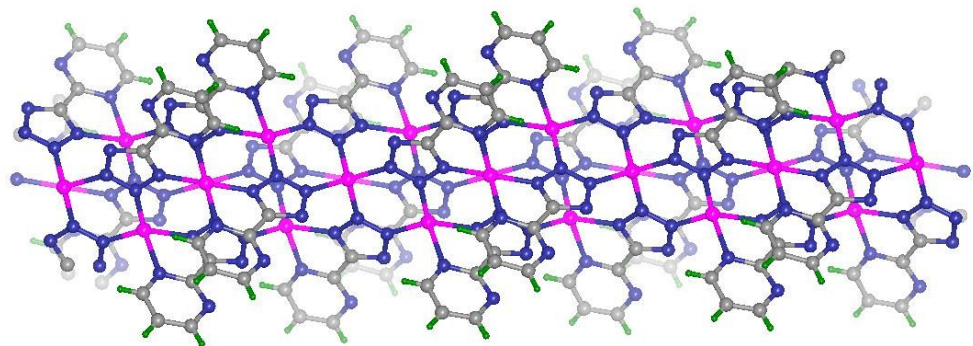


Figure S9. Top left: Coordination mode of *pmtz* ligand and coordination environment of Cu^{II} in **6R** ($\text{Cu}_4(\text{pmtz})_4$). Top right: Top view of the 1D chain structure in **6R**. Bottom: Side view of the 1D chain structure in **6R** (Cu, purple; C, grey; H, green, N, dark blue).

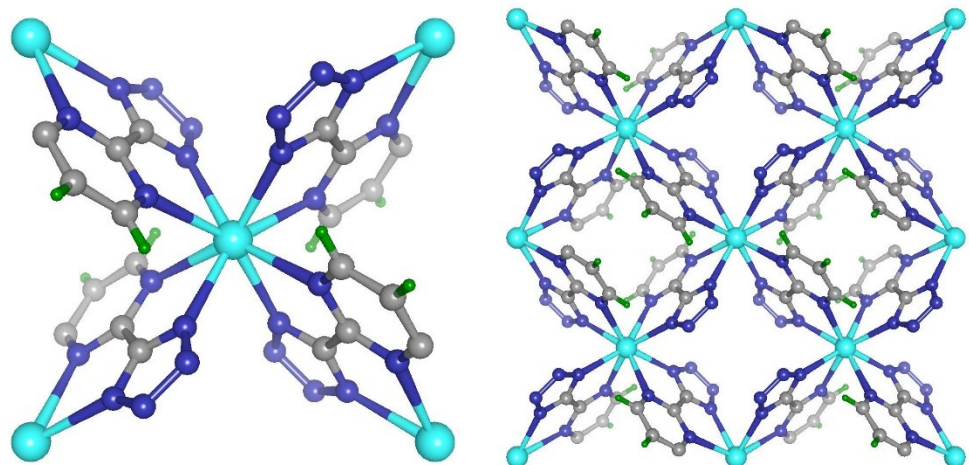


Figure S10. Left: The coordination environment of Cd^{II} and coordination mode of *pmtz* in **7R**, $\text{Cd}(\text{pmtz})_2$. Right: The layer structure in **7R** (Cd, cyan; C, grey; H, green, N, dark blue).

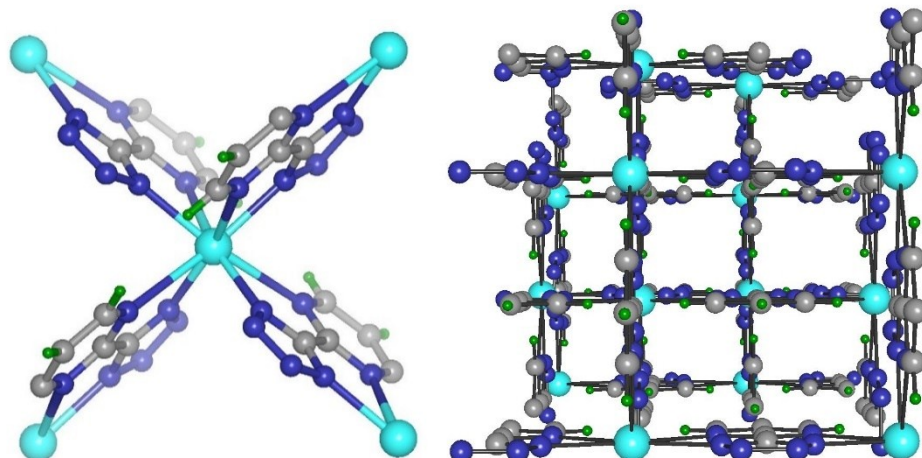


Figure S11. Top left: The coordination environment of Cd^{II} and coordination mode of *pmtz* in **8R**. Top right: The layer structure in **8R**. Bottom: A perspective view of packing of layers in **8R** (Cd, cyan; C, grey; H, green, N, dark blue).

References

- 1 C. Hua, J.-Y. Ge, F. Tuna, D. Collison, J.-L. Zuo and D. M. D'Alessandro, *Dalton Trans.*, 2017, **46**, 2998.
- 2 H.-M. He, Y. Song, F.-X. Sun, N. Zhao and G.-S. Zhu, *Cryst. Growth Des.*, 2015, **15**, 4, 2033.
- 3 M. Dincă, A. Dailly, C. Tsay and J. R. Long, *Inorg. Chem.*, 2008, **47**, 1, 11.
- 4 E. D. Bloch, W. L. Queen, M. R. Hudson, J. A. Mason, D.-J. Xiao, L. J. Murray, R. Flacau, C. M. Brown and J. R. Long, *Angew. Chem. Int. Ed.*, 2016, **55**, 8605.
- 5 M. Dincă, A. Dailly, Y. Liu, C. M. Brown, D. A. Neumann and J. R. Long, *J. Am. Chem. Soc.*, 2006, **128**, 16876.
- 6 M. Dincă, W.-S. Han, Y. Liu, A. Dailly, C. M. Brown and J. R. Long, *Angew. Chem. Int. Ed.*, 2007, **46**, 1419.
- 7 K. Sumida, S. Horike, S. S. Kaye, Z. R. Herm, W. L. Queen, C. M. Brown, F. Grandjean, G. J. Long, A. Dailly and J. R. Long, *Chem. Sci.*, 2016, **1**, 184.
- 8 J.-H. Liao, W.-T. Chen, C.-S. Tsai and C.-C. Wang, *CrystEngComm.*, 2013, **15**, 3377.
- 9 D.-J. Xiao, M. I. Gonzalez, L. E. Darago, K. D. Vogiatzis, E. Haldoupis, L. Gagliardi and J. R. Long, *J. Am. Chem. Soc.*, 2016, **138**, 7161.
- 10 C. K. Brozek, A. F. Cozzolino, S. J. Teat, Y.-S. Chen and M. Dincă, *Chem. Mater.*, 2013, **25**, 2998.
- 11 A. L. Myers and J. M. Prausnitz, *AICHE J.*, 1965, **11**, 121.